Bridge Pressure Flow Scour in Clear Water

Junke Guo[1], Kornel Kerenyi[2], and Jorge E. Pagan-Ortiz[3]

Abstract: Bridge pressure flow scour in clear water is studied analytically and experimentally. The flume experiments with three different decks reveal that: 1) the measured scour profiles under a bridge are more or less 2-dimensional; 2) all the measured scour profiles can be described by two empirical similarity equations, where the horizontal distance is scaled by the deck width while the local scour depth by the maximum scour depth; 3) the maximum scour position is under the bridge about 15% deck width from the downstream deck edge; 4) the scour begins at about one deck width upstream the bridge while the deposition occurs at about 2.5 deck widths downstream the bridge; and 5) the maximum scour depth increases as the bridge opening decreases, but a general relationship for the maximum scour depth must be aided with an analytical study. The analytical study shows that: 1) bridge scour can be divided into three cases: downstream unsubmerged, partially submerged, and totally submerged; 2) for downstream unsubmerged flows, the maximum scour depth is an open-channel problem where methods in terms of critical velocity or bed shear stress can be applied, but this case is only a transition to submerged flows; 3) for partially and totally submerged flows, the equilibrium maximum scour depth can be described by a linear relationship between a geometric similarity number and an inundation similarity number, which has been confirmed with the experimental data. For application, a design and field evaluation procedure with an example is presented, including the maximum scour depth and scour profile.

Keywords: bridge decks, bridge design, bridge foundations, bridge hydraulics, bridge inundation, bridge scour, pressure flows, pressure scour, submerged flows.

[1]Assistant Professor, Dept. of Civil Engineering, Univ. of Nebraska-Lincoln, PKI 204D, 1110 S 67th ST, Omaha, NE 68182-0178. Email: jguo2@unl.edu

[2]Research Hydraulic Engineer, Office of Infrastructure R&D, Turner-Fairbank Highway Research Center, Federal Highway Administration, 6300 Georgetown Pike, McLean, VA 22101. E-mail: kornel.kerenyi@fhwa.dot.gov

[3]Leader of National Hydraulics Team, Office of Bridge Technology, Federal Highway Administration, 1200 New Jersey Avenue SE, Washington, DC 20590. E-mail: jorge.pagan@fhwa.dot.gov

Introduction

Bridge is one of the major crossings in road transportation systems. Bridge flows are usually designed to be open channel flow; it nevertheless becomes pressure flow if the bridge downstream is partially or totally submerged during large floods. Unlike open channel flow, pressure flow has a strong scourbility because to pass a given discharge, the flow can only scour the channel bed.

Due to its strong scourbility, pressure flow scour is very important in the design of bridge foundations. Poor understanding of pressure flow scour will lead to an inappropriate foundation design, which either significantly increases the cost of a project or results in an unsafe infrastructure. Our current knowledge of the pressure flow scour cannot ensure an efficient design that is safe and economical because most of the previous predictors were derived from free surface flows.

To better understand pressure flow scour, three systematic studies were reported in literature. Based on the dataset of Colorado State and using a dimensional analysis, Arneson and Abt (1998) proposed the following multiple linear regression equation

$$\frac{y_s}{h_u} = -0.93 + 0.23\left(\frac{h_u}{h_b}\right) + 0.82\left(\frac{y_s + h_b}{h_u}\right) + 0.03\left(\frac{V_a}{V_c}\right) \tag{1}$$

where y_s = maximum scour depth, h_u = depth of the headwater, h_b = bridge opening before the scour, V_a = velocity under the bridge before scour, and V_c = critical velocity in the headwater

$$V_c = 1.52\sqrt{g\,(s-1)\,d_{50}}\left(\frac{h_u}{d_{50}}\right)^{1/6} \tag{2}$$

where g = gravitational acceleration, s = specific gravity of sediment, and d_{50} = median diameter of the bed materials. Arneson and Abt concluded that the ratio $(y_s + h_b)/h_u$ is the most significant independent, and the ratio V_a/V_c the least. Although Eq. (1) has been adopted in the FHWA manual (Richardson and Davis 2001), it has a serious problem. As Lyn (2005) stated, the ratio $(y_s + h_b)/h_u$ is not appropriate to be an independent since y_s/h_u and $(y_s + h_b)/h_u$ in Eq. (1) are almost self-correlated. Lyn further proposed the following power law

$$\frac{y_s}{h_u} = \min\left[0.091\left(\frac{V_a}{V_c}\right)^{2.95}, 0.5\right] \tag{3}$$

where the critical velocity V_c is estimated by Eq. (2). As a result, Lyn believed that the ratio V_a/V_c governs the pressure flow scour.

The third important study of pressure flow scour is by Umbrell et al. (1998) who did a series of flume experiments in the FHWA Hydraulics Lab. Using the mass conservation and assuming a critical velocity under the bridge, they presented the following equation

$$\frac{y_s + h_b}{h_u} = \frac{V_u}{V_c}\left(1 - \frac{b}{h_u}\right) \tag{4}$$

where V_u = velocity of the headwater, and b = thickness of the bridge deck including girders. By comparing Eq. (4) with their experimental data, Umbrell et al. modified Eq. (4) as

$$\frac{y_s + h_b}{h_u} = 1.102\left[\frac{V_u}{V_c}\left(1 - \frac{b}{h_u}\right)\right]^{0.603} \tag{5}$$

where the critical velocity is estimated by Eq. (2) except the coefficient 1.52 is replaced by 1.58. The question is that the critical velocity equation (2), is derived from the Manning equation and a critical Sheilds number (Richardson and Davis 2001, Appendix C), which is only valid when the under bridge flow is uniform open-channel flow. In other words, Eq. (4) or (5) should not be valid when a bridge downstream is submerged since such a flow is rapidly varied pressure flow.

To sum up, all the previous studies did not give any information about the scour range along the river. In particular, the irony is that when they studied *pressure* flow scour, they never considered the effect of pressure under the bridge deck anyway. This ignorance is a serious problem in understanding the mechanism and formulating an equation of bridge pressure flow scour.

The objectives of this study are then twofold: to understand the mechanism of bridge pressure flow scour, and to determine a solution for pressure flow scour. Specifically, (1) we start with a series of flume experiments that are used to examine the existing methods and test a new hypothesis on bridge pressure flow scour. (2) We divide bridge flows into three cases and apply the mass and energy conservation laws to each case, which leads to hypotheses for pressure flow scour predictions. The hypotheses are then tested with the flume experimental data. (3) For application, we present a procedure for calculating the maximum scour depth and scour profile.

Experimental Study

The objective of this experimental study is to collect bridge scour data under controlled flow conditions. The collected data can then be used to formulate a general understanding of bridge pressure flow scour, and to test the existing prediction equations and a new hypothesis proposed in this

paper. To this end, we conducted a series of flume experiments in the FHWA Hydraulics Laboratory, located at the Turner-Fairbank Highway Research Center in McLean, VA. The experimental set-up, results, data analysis and interpretation are described as follows.

Experimental set-up

Flume system: Fig. 1a shows an overview of the experimental flume; and Fig. 1b details the flume system. The flume is rectangular, 21.35 m long and 1.83 m wide with glass sides and stainless steel bottom. As shown in Fig. 1b, in the middle of the flume was installed a test section 0.63 m wide and 2.8 m long, together with a model bridge deck. A honeycomb flow straightener and a trumpet-shaped inlet were carefully designed to smoothly guide the flow into the test channel. Referring to the side view in Fig. 1b, a 40-cm sediment recess, which is amplified in Fig. 2, on the flume bottom and under the bridge was installed for local scour information. The flume was set horizontally, and an adjustable tailgate located at the downstream end of the flume controlled the depth of flow. A circulation system with a sump and a pump supplied water in the flume. The capacity of the sump was 210 m^3 while the pump output rate could vary between 0 and 0.3 m^3/s. An electromagnetic flowmeter was used to measure the discharge. More information about the flume can be found at: http://www.fhwa.dot.gov/engineering/hydraulics/research/lab.cfm.

Sand bed preparation: Fig. 2 shows the sand bed preparation in the test channel. The median bed material diameter was $d_{50} = 1$ mm; a 20-cm thick layer of sand was distributed evenly on the flume bottom. The sediment recess on the flume bottom could model a local scour depth til 60 cm.

Model decks: Three model decks, made of special Plexiglas and shown in Fig. 3, were used in the experiments. The 6-girder deck was chosen since most US highway bridges with 4-lanes have 6-girders, while the 3-girder deck corresponds to bridges with 2-lanes. Both the 6-girder and 3-girder decks have rails, shown in Fig.3a, which can pass overflow on the deck surface. For comparison, a streamline deck was also tested since it has the least scour depth. The deck elevation was adjustable, permitting the deck to have 8 bridge openings.

Operating discharge: This study emphasizes clear water scour since it is usually larger than the corresponding live bed scour. To ensure a clear water scour under the bridge, the approach velocity in the test channel must be less than the critical velocity, which can be estimated by Eq. (2). Since the flow depths in the experiments were always kept 25 cm, according to Eq. (2), the critical velocity is about

$$V_c = 0.485 \text{ m/s}$$

which corresponds to a maximum allowable discharge in the test channel

$$Q_{\max} = (0.485\,\mathrm{m/\,s})\,(0.63\,\mathrm{m})\,(0.25\,\mathrm{m}) = 0.0764\ \mathrm{m^3/s} = 76.4\ \mathrm{l/\,s}$$

where 0.63 m is the width of the test section. The operating discharge was then chosen as 64.6 l/ s, corresponding to an approach velocity $V_u = 0.41\,\mathrm{m/\,s}$, Reynolds number $\mathrm{Re} = V_u h_u/\nu = 2.3 \times 10^5$ where ν = kinematic viscosity of water, and Froude number $\mathrm{Fr} = V_u/\sqrt{g h_u} = 0.35$.

Data collection: An automated flume carriage fitted to the main flume, shown in Fig. 4, was used to collect scour data which were measured using a laser distance sensor. A LabVIEW was applied for data acquisition, instrument control, data analysis, and report generation.

Experimental procedures: 1) Made the sediment bed in the test section like that in Fig. 2; 2) installed a bridge deck and positioned it perpendicular to the direction of flow; 3) adjusted the elevation of the deck to a designed bridge opening; 4) pumped water from the sump to the flume gradually from 0 to 64.6 l/ s, which could be checked with the electromagnetic flowmeter; 5) run each experiment for 36-48 hours so that the scour profile could reach its equilibrium state; and 6) mapped the 3-dimensional scour hole using the laser distance sensor.

Experimental results

The major results are the 3-dimensional scour mapping records, which can be downloaded at http://myweb.unomaha.edu/~junkeguo/ or http://www.fhwa.dot.gov/engineering/hydraulics/. We present them only in 3-dimensional visualization, longitudinal profiles, and maximum scour depth.

Fig. 5 represents a 3-dimensional scour hole, which clearly shows a more or less uniform scour in the lateral direction. In other words, the scour holes under the bridge are approximately 2-dimensional. Fig. 6 then plots all the width-averaged scour profiles under both the 3-girder and the 6-girder decks, where $x = 0$ is defined at the maximum scour point that is 4 cm from the downstream deck edge. We can see that: 1) the scour profiles are about bell-shaped curves, but they are not symmetrical because the eroded materials deposit about 2-3 deck widths downstream the bridge where $y > 0$; and 2) the scours begin at about one deck width upstream the bridge. The most important results, the maximum scour depths, are tabulated in Table 1 in column 2, which shows that the maximum scour depths increase as the bridge openings in column 1 decrease.

Data analysis and interpretation

Similarity of scour profiles: By looking at all the profiles in Fig. 6, we hypothesize that a similarity profile may exist by scaling the horizontal length x with the deck width W, and the local scour y with the maximum value y_s. Fig. 7 replots the scour profiles according to y/y_s versus x/W, which shows that before the maximum scour point $x \leq 0$, all measured profiles collapse into a single curve; after the maximum scour point, $x > 0$, the measured profiles fall into a single curve, but data are somewhat scatter because the flow becomes open-channel flow.

For the scour profiles under the 3-girder deck, shown in Fig. 7a, the similarity profile for $x \leq 0$ is well fitted by

$$\frac{y}{y_s} = -\exp\left(-\left|\frac{x}{W}\right|^{2.5}\right) \tag{6}$$

For $x > 0$, it can be approximated by

$$\frac{y}{y_s} = -1.055\exp\left[-\frac{1}{2}\left(\frac{x}{W}\right)^{1.8}\right] + 0.055 \tag{7}$$

Eqs. (6) and (7) are also plotted in Fig. 7a. To check the universality of Eqs. (6) and (7), we also plot them in Fig. 7b where again excellent agreement with the flume data is clearly observed.

Interpretation: Eqs. (6) and (7) can be interpreted in the initiation of scour and deposition. Defining a scour initiation at $y/y_s = -0.01$ in Eq. (6), its position x_s is then determined by

$$-0.01 = -\exp\left(-\left|\frac{x_s}{W}\right|^{2.5}\right) \tag{8}$$

This gives

$$\frac{x_s}{W} = -1.842 \tag{9}$$

which is shown in Fig. 8. Considering the upstream deck edge is at

$$\frac{x}{W} = -\frac{26\,\text{cm} - 4\,\text{cm}}{26\,\text{cm}} = -0.846\,15 \tag{10}$$

which is also shown in Fig. 8, the relative distance between the scour initiation and the upstream deck edge is

$$\frac{x - x_s}{W} = -0.846\,15 - (-1.842) = 0.995\,85 \approx 1 \tag{11}$$

which means the scour begins at about one deck width upstream the bridge.

The deposition position x_d can be clearly defined by $y/y_s = 0$ in Eq. (7), which gives

$$\frac{x_d}{W} = 2.682\,7 \tag{12}$$

Considering the downstream deck edge is at

$$\frac{x}{W} = \frac{4\,\text{cm}}{26\,\text{cm}} = 0.153\,85 \tag{13}$$

the relative distance between the downstream deck edge and the deposition point is

$$\frac{x_d - x}{W} = 2.682\,7 - 0.153\,85 = 2.528\,9 \tag{14}$$

which means the deposition begins at about 2.5 deck widths downstream the bridge.

Similarly, Eqs. (6) and (7) give the relative scour depths at the two deck edges

$$\left.\frac{y}{y_s}\right|_{\text{upstream edge}} = 0.518, \quad \text{and} \quad \left.\frac{y}{y_s}\right|_{\text{downstream edge}} = 0.985 \tag{15}$$

This is useful for scour evaluation practice, which is further detailed in an example later. For intuition, Fig. 8 gives a normalized scour profile with various characteristics.

In brief, the horizontal range of a pressure flow scour depends on the width of bridge deck. Nevertheless, the design of a scour profile by Eqs. (6) and (7) needs the maximum scour depth y_s.

Determination of the maximum scour depth using the existing methods: The three existing methods mentioned in the introduction are tested in Fig. 9 where overflow has been subtracted according to Umbrell et al. (1998). We can see that the Arneson and Abt method has an adverse tendency with the experimental data, which means the functional structure of their equation is not correct; and Lyn's method systematically overestimates the present data. Although the Umbrell et al. method is the best in the existing methods, in terms of application, none of them provides reliable predictions. As we commented in the introduction, the heritage problem of the existing methods is that they never considered the pressure effect under the bridge.

In the following section, we will provide an analytical method for estimating the maximum scour depth y_s, by applying the mass and energy conservation laws where the effect of streamline curvature under the bridge is included.

Analytical Study of Maximum Scour Depth

The present experiments were conducted under one velocity condition, but the purpose of the experiments is to make the results as widely applicable as possible. To achieve this end, a similarity equation including the approach velocity for the maximum scour depth must be established.

For clarification, we state the problem as: **Given** a bridge crossing over a steady river flow with clear water, shown in Fig. 10 where without contraction channel and piers, V_u = velocity of the upstream flow, B = width of the river, W = width of the bridge deck, d_{50} = median diameter of the bed materials, h_u = depth of the headwater, h_b = bridge opening before scour, and b = thickness of the bridge deck including girders. **Find** the equilibrium maximum scour depth y_s in Fig. 10b, c and d by considering a unit river flow.

Flow Classification

The solution to the problem depends on the tailwater surface elevation. By analogy to culvert flows (Gupta 2008, p.778), we can divide bridge flows into three cases:

Case 1: If the downstream low chord of a bridge is unsubmerged, shown in Fig. 10b, the bridge operates as an inlet control sluice gate. The scour is independent of the bridge width and continues until a uniform flow and a critical bed shear stress reach. This case only occurs for upstream slightly submerged, say, $h_u/h_b < 1.1$, but it often becomes downstream submerged before an equilibrium scour reaches. This case is unrelated to the present experiments, we leave it in Appendix A.

Case 2: If the downstream low chord of a bridge is partially submerged, shown in Fig. 10c, the bridge operates as an outlet control orifice, and the flow under the bridge is rapidly varied pressure flow. This case occurs when $h_u/h_b \geq 1.1$, which is explained at the end of this section.

Case 3: If the bridge is totally submerged, shown in Fig. 10d, it operates as the combination of an orifice and a weir; only the discharge under the bridge affects scour depth. We will only emphasize the solutions for Cases 2 and 3 in the following.

Case 2: Partially Submerged Flows

Cases 2 and 3 are rapidly varied pressure flows. Referring to Fig. 10c, if an energy equation is applied to the streamline 1-2, we have

$$h_u + \frac{\alpha_1 V_u^2}{2g} = h_b + \frac{p_2}{\gamma} + \frac{\alpha_2 V_b^2}{2g} + K_b \frac{V_u^2}{2g} \tag{16}$$

where the pressure p_2 at point 2 is not hydrostatic and must be solved from the Bernoulli equation across streamlines. Referring to Eq. (B-9) in Appendix B, we have

$$\frac{p_2}{\gamma} = \beta\left(h_u - h_b\right) - K_p\frac{V_b^2}{2g} \tag{17}$$

where $\beta > 1$ because point 2 is slightly lower than the bottom of girders; and $K_p < 1$ because the radius of curvature at the maximum scour point, in Eq. (B-8), is very large. The last term in Eq. (17) is called a curvature pressure due to centrifugal acceleration at point 2. Eq. (17) shows that the curvature pressure under the bridge is negative, which is consistent with our recent measurements on lift of an inundated bridge deck (Kornel et al. 2008) where the lift points downward.

The bed shear stress at the maximum scour point is the critical shear stress, described by Eq. (A-2) in Appendix A. However, the critical shear stress is uncoupled with the energy equation (16) where the friction loss is neglected. This implies that the effect of critical shear stress or sediment size can be neglected if an equilibrium scour reaches. The previous studies took critical velocity or shear stress as one of the major independents because they were purely based on dimensional analysis (Arneson and Abt 1998, Lyn 2005) or continuity equation (Umbrell et al. 1998).

Substituting Eq. (17) into Eq. (16) and rearranging it gives

$$\left(\alpha_2 - K_p\right)\frac{V_b^2}{2g} = \left(1-\beta\right)\left(h_u - h_b\right) + \left(\alpha_1 - K_b\right)\frac{V_u^2}{2g} \tag{18}$$

Referring to Fig. 10c and applying the continuity equation

$$V_b\left(h_b + y_s\right) = V_u h_u \tag{19}$$

to Eq. (18) and rearranging it gives

$$\left(\frac{h_u}{h_b + y_s}\right)^2 = -\frac{2\left(\beta-1\right)}{\alpha_2 - K_p}\frac{g\left(h_u - h_b\right)}{V_u^2} + \frac{\alpha_1 - K_b}{\alpha_2 - K_p} \tag{20}$$

Defining a deck block depth as $a = h_u - h_b$ in Fig. 10c, Eq. (20) can be rewritten as

$$\left(\frac{h_b + a}{h_b + y_s}\right)^2 = -\frac{2\left(\beta-1\right)}{\alpha_2 - K_p}\frac{g\left(h_u - h_b\right)}{V_u^2} + \frac{\alpha_1 - K_b}{\alpha_2 - K_p} \tag{21}$$

in which $h_u - h_b$ on the right-hand-side is kept in order to compare it with the solution for Case 3.

From Eq. (21) we can make the following hypotheses:

1. The pressure flow scour can be described with a geometric number, $(h_b + a)^2 / (h_b + y_s)^2$, and an inundation number, $g(h_u - h_b)/V_u^2$.

2. Given a deck shape, the experimental data will fall into a straightline according to Eq. (21).

3. Both the slope and intercept in Eq. (21) varies with deck shapes, but the slope must be negative while the intercept positive. The slope is negative because $\beta > 1$, $\alpha_2 > 1$ and $K_p < 1$. The intercept must be positive because when $h_u \to h_b$, we have $y_s \to 0$, which gives

$$\left(\frac{h_b + a}{h_b}\right)^2 = \frac{\alpha_1 - K_b}{\alpha_2 - K_p} > 0 \tag{22}$$

4. The equilibrium scour depth is independent of sediment size because Eq. (21) does not include critical shear stress or sediment size. This hypothesis cannot be directly tested with the present experiments, but experiments with different sediment sizes will be added in the near future. We will test hypotheses 1-3 after discussing the solution for Case 3.

Case 3: Totally Submerged Flow

The solution for Case 2 can be adapted to Case 3 if the deck block depth a on the left-hand-side of Eq. (21) is replaced with the deck thickness b, shown in Fig. 10d. This can be proved by applying the energy equation (16) to Fig. 10d and considering the discharge under the bridge.

When Eq. (16) is applied to Fig. 10d, the pressure p_1 is hydrostatic, and the pressure p_2 is the same as that in Eq. (17). Following Umbrell et al. (1998), the overflow velocity is approximated to be the same as the upstream velocity V_u, which results in the unit discharge q_1 under the bridge

$$q_1 = V_u (h_b + b) \tag{23}$$

and the corresponding velocity at the maximum scour section

$$V_b = \frac{h_b + b}{h_b + y_s} V_u \tag{24}$$

Substituting Eq. (24) into Eq. (18) and rearranging it gives

$$\left(\frac{h_b + b}{h_b + y_s}\right)^2 = -\frac{2(\beta - 1)}{\alpha_2 - K_p} \frac{g(h_u - h_b)}{V_u^2} + \frac{\alpha_1 - K_b}{\alpha_2 - K_p} \tag{25}$$

which is the same as Eq. (21) except the deck block depth a is replaced with the deck thickness b. In general, we can unify Cases 2 and 3 with Eq. (21) where

$$a = \min\{h_u - h_b, b\} \tag{26}$$

Maximum Scour Depth

Now we can determine the maximum scour depth y_s from Eq. (21) and the experimental data in Table 1. For simplicity, we denote the inundation number as

$$X = \frac{g(h_u - h_b)}{V_u^2} \tag{27}$$

which includes the approach velocity or Froude number, and the geometric number as

$$Y = \left(\frac{h_b + a}{h_b + y_s}\right)^2 \tag{28}$$

Eq. (21) then becomes

$$Y = mX + c \tag{29}$$

where

$$m = -\frac{2(\beta - 1)}{\alpha_2 - K_p} \quad \text{and} \quad c = \frac{\alpha_1 - K_b}{\alpha_2 - K_p} \tag{30}$$

To test the linear relationship, Eq. (21) or (29), the inundation number X and the geometric number Y for the experimental data are listed in Table 1 in columns 4 and 5, respectively, which are then plotted in Fig. 11. As expected in Eq. (21), i) the pressure flow scour can be described with the geometric number, $Y = (h_b + a)^2 / (h_b + y_s)^2$, and the inundation number, $X = g(h_u - h_b)/V_u^2$; ii) the experimental data fall into a straightline according to Y versus X, i.e.

$$Y = -0.0551X + 1.2115 \tag{31}$$

and iii) the slope and intercept are, respectively,

$$m = -0.0551 \quad \text{and} \quad c = 1.2115 \tag{32}$$

These results confirm our hypotheses based on the mass and energy conservation laws. Eq. (31) is

the major result of this study. Besides, the data of the 3-girder and the 6-girder decks almost fall into a single straightline, which means the scour is independent of the number of girders. This is because flow separates from the bridge at the upstream girder, and becomes open-channel flow at about the downstream deck edge. The girders after the first one do not interact with the core flow directly, as shown in Fig. 10c and d.

For a streamline deck, which will be added later, we expect that the slope m must be smaller than that of the 3-girder and 6-girder decks since both β and K_p become smaller. The intercept c may be larger or smaller, depending on the relative reductions of K_b and K_p.

Criteria for Cases 1 and 2

Clearly, the criterion for Case 3 is when an overflow occurs. The criteria for Cases 1 and 2 are derived here. Since

$$\frac{h_u}{h_b} \geq \frac{h_u}{h_b + y_s} \tag{33}$$

and the maximum value of $h_u/\left(h_b + y_s\right)$ can be found from Eqs. (28) and (31)

$$\left.\frac{h_u}{h_b + y_s}\right|_{\max} = \sqrt{1.2115} \approx 1.1 \tag{34}$$

where $h_u = h_b + a$ for Case 2 has been considered, we then have the criterion for Case 2

$$\frac{h_u}{h_b} \geq 1.1 \tag{35}$$

In other words, Case 1 occurs when $h_u/h_b < 1.1$. This is similar to the condition of unsubmerged culvert where $h_u/h_b < 1.2$, and submerged culvert where $h_u/h_b \geq 1.2$ (Gupta 2008, p778).

To summarize this section, we state that: i) Case 2 occurs when $h_u/h_b \geq 1.1$; ii) Cases 2 and 3 can be unified with Eq. (31); iii) once the maximum scour depth is estimated by Eq. (31), the scour profile can be calculated by Eqs. (6) and (7).

The application of the present study can be summarized through a design procedure.

Design Procedure and Application Example

Given a design unit discharge q, bridge opening h_b, deck thickness b, and bed material diameter d_{50}, find the scour depth y_s and scour profile. The design procedure is like this:

Step 1: Use HEC-RAS for gradually varied flows or the Manning equation for uniform flows to estimate the upstream flow depth h_u.

Step 2: Check if a clear water scour occurs in the upstream flow according to Eq. (2). If the upstream velocity V_u is greater than the critical velocity V_c, a procedure for live bed scour should be used, but a design with clear water is more conservative.

Step 3: Classify the flow case according to Eq. (35).

Step 4: Calculate the deck block depth a by Eq. (26).

Step 5: Calculate the inundation similarity number, X, from Eq. (27).

Step 6: Calculate the geometric similarity number, Y, from Eq. (31), and the maximum scour depth, y_s, from Eq. (28)

$$y_s = \frac{h_b + a}{\sqrt{Y}} - h_b \tag{36}$$

Step 7: Plot the design scour profile according to Eqs. (6) and (7).

To check the accuracy of Eq. (31), the calculated scour depth for each experimental run, according to the above steps, is tabulated in Table 1 in column 6, and the corresponding relative error in column 7, which shows that except for 4 runs, most calculated errors are less than 10%, which is usually within measurement uncertainties. For comparison with the previous studies, Fig. 12 plots the measured and calculated values according to columns 2 and 6 in Table 1.

Example 1 (Foundation Design): This example is modified from HEC-18 (Richardson and Davis 2001, p6.32). An existing bridge, with a deck width $W = 10\,\mathrm{m}$ supported by 3 girders, is subjected to pressure flow to the top of a solid guard rail at the 100-year flood. There is only a small increase in flow depth at the bridge for the 500-year flood due to the large overbank area. The bed materials are $d_{50} = 0.4\,\mathrm{mm}$, and the bridge opening is $h_b = 7.93\,\mathrm{m}$ before scour. Calculate the vertical contraction scour.

Step 1: According to HEC-18, a HEC-RAS model with 500-year flood gives

$$h_u = 9.75\,\mathrm{m}, \quad V_u = 2.93\,\mathrm{m/s}, \quad q = 28.56\,\mathrm{m^2/s}$$

Step 2: According to Eq. (2), the critical velocity is

$$V_c = 1.52\sqrt{(1.98)\,(1.65)\,(0.0004)}\left(\frac{9.75}{0.0004}\right)^{1/6} = 0.295\,87\,\mathrm{m/s}$$

which means this is a live bed scour, which is smaller than a clear water scour. However, for safety, we design it with clear water condition.

Step 3: According to the problem statement, there is only a small increase in flow depth so that we assume no overflow occurs. This gives the ratio

$$\frac{h_u}{h_b} = \frac{9.75}{7.93} = 1.2295 > 1.1$$

According to Eq. (35), the flow is in Case 2. Thus, Eq. (31) is used to estimate the maximum scour depth.

Step 4: The deck block depth is then

$$a = h_u - h_b = 9.75 - 7.93 = 1.82\,\text{m}$$

Step 5: The inundation number is

$$X = \frac{g\,(h_u - h_b)}{V_u^2} = \frac{(9.81)\,(1.82)}{2.93^2} = 2.0797$$

Step 6: From Eq. (31) the geometric number is

$$Y = -0.0561\,(2.0797) + 1.191 = 1.0743$$

According to Eq. (28), the maximum scour depth is then solved from Eq. (36)

$$y_s = \frac{7.93 + 1.82}{\sqrt{1.0743}} - 7.93 = 1.4768\,\text{m}$$

which, from Eq. (13), is at a distance from the downstream deck edge

$$x_0 = 0.152W = (0.152)\,(10.4) = 1.5808\,\text{m}$$

For comparison, HEC-18 gives $y_s \approx 11\,\text{m}$ without specifying the locus.

Step 7: The equilibrium scour profile is then estimated by Eqs. (6) and (7), which become

$$y = -1.4768 \exp\left(-\left|\frac{x}{10}\right|^{2.5}\right)$$

for $x \leq 0$, and

$$\begin{aligned} y &= -(1.4768)(1.055)\exp\left[-\frac{1}{2}\left(\frac{x}{10}\right)^{1.8}\right] + (0.055)(1.4768) \\ &= -1.558\exp\left[-\frac{1}{2}\left(\frac{x}{10}\right)^{1.8}\right] + 0.081224 \end{aligned}$$

for $x > 0$. The equilibrium scour profile is shown in Fig. 13.

Example 2 (Scour Evaluation): For a field scour evaluation for the above example, if we measured the scour depth at the upstream deck edge is about

$$y|_{\text{upstream deck edge}} = 0.764\,\text{m}$$

according to Eq. (15), the corresponding maximum scour depth is about

$$y_s = \frac{0.764}{0.518} = 1.4749\,\text{m}$$

Comparing this with the design foundation, we know wether or not the scour is critical.

Conclusions

The following conclusions can be drawn from the present study:

The experiments show that: 1) the horizontal range of a bridge pressure flow scour only depends on the deck width; the scour starts at about one deck width upstream the bridge, as seen in Eq. (11), and the deposition starts at about 2.5 deck widths downstream the bridge, as seen in Eq. (14); and 2) a similarity scour profile exists, where the horizontal length is scaled by the deck width, and the vertical by the maximum scour depth, shown in Eqs. (6) and (7).

The analytical study show that: 1) the maximum scour depth can be described by a linear relationship, Eq. (31), between the inundation number and the geometric number, which has been confirmed the experimental data in Fig. 11; 2) the maximum scour depth is independent of the number of girders; 3) the maximum scour depth is independent of sediment size, but this needs to be further tested by experiments with different sediment sizes; and 4) submerged scours occur only if the ratio of the headwater depth to the bridge opening is equal to or greater than 1.2, as described by Eq. (35).

This study can be used to evaluate an existing bridge scour and to design a new bridge foun-

dation. For evaluation, once we measure the scour depth at the upstream or downstream edge, we can convert them to the maximum scour depth according to Eq. (15) or Fig. (8). For design, once we calculate the maximum scour depth from Eq. (31), we can estimate the scour profile from Eqs. (6) and (7), as described by the examples.

Acknowledgement

This research was supported by the Federal Highway Administration's Hydraulics R&D Program with Contract No. DTFH61-04-C-00037.

Appendix A: Maximum Scour Depth for Case 1

Referring to Fig. 10b, when the scour reaches its equilibrium state, the downstream flow is uniform with a critical bed shear stress. If the uniform flow is described by the Manning equation, and the critical bed shear stress is described by the Shields diagram, the downstream flow depth is exactly the same as that in clear water contraction scour (Richardson and Davis 2001, p.C.5)

$$h = \left[\frac{nq^2}{(s-1)\, d_{50}\tau_{c*}}\right]^{3/7} \tag{A-1}$$

where h = downstream flow depth, n = Manning coefficient, q = unit discharge, and the critical Shields number τ_{c*} can be found by the following equation (Guo 1990, 1997, 2002)

$$\tau_{c*} = \frac{0.23}{d_*} + 0.054\left[1 - \exp\left(-\frac{d_*^{0.85}}{23}\right)\right] \tag{A-2}$$

in which

$$\tau_{c*} = \frac{\tau_c}{(s-1)\,\gamma d_{50}} \tag{A-3}$$

where τ_c = critical bed shear stress, and the dimensionless diameter d_* is defined as

$$d_* = d_{50}\left[\frac{(s-1)\, g}{\nu^2}\right]^{1/3} \tag{A-4}$$

where ν = kinematic viscosity of water.

With the downstream flow depth h available, the scour depth y_s can be found by the energy

equation between points 1 and 2 in Fig. 10b where the datum is chosen at the maximum scour bed

$$y_s + h_u + \frac{\alpha_1 V_u^2}{2g} = h + \frac{\alpha_2 V_b^2}{2g} + K_b \frac{V_b^2}{2g} \tag{A-5}$$

where α_1 and α_2 are energy correction coefficients, K_b = entrance energy loss coefficient, which can be taken as 0.52 according to a box culvert experiment (Jones et al. 2006). Note that the energy loss due to friction has been neglected because of the short distance between points 1 and 2.

The scour depth from Eq. (A-5) is then

$$y_s = h - h_u + \frac{q^2}{2gh^2}\left[\alpha_2 + K_b - \alpha_1 \left(\frac{h}{h_u}\right)^2\right] \tag{A-6}$$

where $V_u = q/h_u$ has been used.

Theoretically, Case 1 is well defined with Eqs. (A-1)-(A-6). Practically, Case 1 is only a short transition to Case 2. This is because if the upstream submerged is not significant, $h_u/h_b < 1.1$, as scour develops, the eroded materials will deposit somewhere downstream the bridge, which then raises the tailwater and makes the downstream deck submerged.

Appendix B: Derivation of Pressure under Bridge Deck

The Bernoulli equation across streamlines (Young 2007, p72) is

$$\frac{p}{\gamma} + z + \frac{1}{g}\int \frac{V^2}{\mathcal{R}} dn = \text{ constant across streamlines} \tag{B-1}$$

where $\mathcal{R}$ = local radius of curvature of a streamline, and n = normal coordinate to the streamline and toward concave side. We can simplify the flow through the maximum scour cross-section with circular streamlines and constant velocity V_b, as shown in Fig. 14. Applying Eq. (B-1) to the vertical line gives

$$\frac{p}{\gamma} + z + \frac{1}{g}\int_0^z \frac{V_b^2}{R_0 - z} dz = \text{const} \tag{B-2}$$

where the coordinates n and z are coincident in the vertical through the maximum scour point, R_0 = local radius at the maximum scour point as shown in Fig. A-1, and the local radius $\mathcal{R} = R_0 - z$ at position z has been applied. Integrating Eq. (B-2) gives

$$\frac{p}{\gamma} + z - \frac{V_b^2}{g} \ln \frac{R_0 - z}{R_0} = \text{const} \tag{B-3}$$

Applying Eq. (B-3) to point 2 yields

$$\frac{p_2}{\gamma} + z_2 - \frac{V_b^2}{g} \ln \frac{R_0 - z_2}{R_0} = \text{const} \tag{B-4}$$

which is valid for any velocity at point 2. If $V_b = 0$, from Fig. 10c we have

$$\frac{p_2}{\gamma} = \beta \left(h_u - h_b \right) \tag{B-5}$$

where $\beta > 1$ since point 2 should be slightly lower than the bottom of girders. Substituting Eq. (B-5) and $V_b = 0$ into (B-4) gives the integration constant

$$\text{const} = \beta \left(h_u - h_b \right) + z_2 \tag{B-6}$$

Substituting Eq. (B-6) into (B-4) and rearranging it gives the general equation at point 2

$$\frac{p_2}{\gamma} = \beta \left(h_u - h_b \right) + \frac{V_b^2}{g} \ln \left(1 - \frac{z_2}{R_0} \right) \tag{B-7}$$

Defining a curvature coefficient as

$$K_p = -2 \ln \left(1 - \frac{z_2}{R_0} \right) \tag{B-8}$$

Eq. (B-7) becomes

$$\frac{p_2}{\gamma} = \beta \left(h_u - h_b \right) - K_p \frac{V_b^2}{2g} \tag{B-9}$$

in which the last term is called a curvature pressure. Clearly, the parameter K_p represents the effect of the ratio of the maximum flow depth under the deck to the radius of curvature at the maximum scour point. From Fig. 7, we can see that a similarity scour profile exists for all measured profiles, which means the geometric ratio of z_2/R_0 is a universal constant, which leads to that the curvature coefficient K_p is a universal constant.

Eq. (B-9) is used in Eq. (16) in the text.

Notation

The following symbols are used in this paper:

a	=	deck block depth
B	=	width of a river
b	=	thickness of bridge deck including girders
c	=	intercept in Eq. (29)
d_{50}	=	median diameter of sediment
Fr	=	Froude number
g	=	gravitational acceleration
h	=	downstream flow depth in Case 1
h_b	=	bridge opening
h_u	=	depth of headwater
K_b	=	energy loss coefficient of bridge entrance
K_p	=	curvature pressure coefficient
m	=	slope in Eq. (29)
n	=	Manning coefficient, or normal direction of a streamline
p	=	pressure
$Q_{\max}$	=	maximum allowable discharge in the flume
q	=	unit discharge of a river
q_1	=	unit discharge under the bridge
$\mathcal{R}$	=	local radius of curvature of a streamline
Re	=	Reynolds number
R_0	=	local radius of curvature at the maximum scour point
s	=	specific gravity of sediment
V_a	=	velocity under the bridge before scour
V_b	=	velocity under the bridge at the maximum scour depth
V_c	=	critical velocity
V_u	=	velocity of the headwater
W	=	width of bridge, shown in Fig. 1a
X	=	inundation similarity number
x	=	coordinate along a river
x_0	=	coordinate of the downstream deck edge
Y	=	geometric similarity number
y_s	=	maximum scour depth
z	=	vertical direction in Appendix
α_1, α_2	=	energy correction coefficient
γ	=	specific weight of water
ν	=	kinematic viscosity of water
τ_c	=	critical shear stress
τ_{c*}	=	critical Shields number

References

Arneson, L. A., and Abt, S. R. (1998). "Vertical contraction scour at bridges with water flowing under pressure conditions." *Transportation Research Record.* 1647, 10-17.

Guo, J. (1990). *Basic Laws of Sediment Transport.* Technical Report, Shanxi Provincial Natural Science Foundation, Taiyuan, Shanxi, China (in Chinese).

Guo, J. (1997). "Discussion: Albert Shields Story." *J. Hydraul. Engrg.*, 123(7), 666.

Guo, J. (2002). "Hunter Rouse and Shields Diagram." *Proc. 13th IAHR-APD Congress,* World Scientific, 2, 1096-1098.

Gupta, R. S. (2008). *Hydrology and Hydraulic systems.* 3rd Ed., Waveland Press.

Kerenyi, K., Sofu, T., and Guo, J. (2008). "Modeling hydrodynamic forces on bridge decks using supercomputer." *Public Road,* (in press).

Lyn, D. A. (2005). "Pressure-flow scour: a re-examination of the HEC-18 equation." Proc. ASCE World Environmental and Water Resources Congress 2006, Omaha, NE.

Richardson, E. V., and Davis, S. R. (2001). *Evaluating scour at bridges.* HEC-18, FHWA-NH-01-001, 4th Ed., U.S. Dept. of Transp., Washing, D.C.

Umbrell, E. R., Young, G. K., Stein, S. M., and Jones, J. S. (1998). "Clear-water contraction scour under bridges in pressure flow." *J. Hydraul. Engrg.*, 124(2), 236-240.

Jones, J. S., Kerenyi, K., and Stein, S. (2006). *Effects of Inlet Geometry on Hydraulic Performance of Box Culverts.* FHWA-HRT-06-138, U.S. Dept. of Transp., Washing, D.C.

Table 1: Summary of experimental results

Bridge opening h_b, (cm)	Measured scour depth y_s, (cm)	Block depth a, (cm)	Inundation number X	Geometric number Y	Calculated scour depth y_s, (cm)	Relative error (%)
(1)	(2)	(3)	(4)	(5)	(6)	(7)
		Deck with 3-girders				
21.0	2.77	4.00	2.3343	1.1062	3.02	9.2
19.5	3.98	5.06	3.2097	1.0943	4.65	16.8
18.0	5.18	5.06	4.0851	0.9899	5.22	0.8
16.5	5.45	5.06	4.9604	0.9650	5.76	5.7
15.0	6.35	5.06	5.8358	0.8830	6.27	-1.3
15.0	6.42	5.06	5.8358	0.8773	6.27	-2.4
13.5	6.41	5.06	6.7112	0.8692	6.73	5.0
12.0	6.43	5.06	7.5866	0.8571	7.15	11.3
10.5	7.31	5.06	8.4619	0.7635	7.53	3.0
		Deck with 6-girders				
22.0	1.75	3.00	1.7507	1.1080	1.68	-4.3
20.5	2.99	4.02	2.6261	1.0897	3.24	8.4
20.5	2.98	4.02	2.6261	1.0906	3.24	8.8
19.0	4.23	4.02	3.5015	0.9821	3.81	-9.9
19.0	4.52	4.02	3.5015	0.9580	3.81	-15.7
17.5	4.47	4.02	4.3769	0.9595	4.35	-2.7
16.0	5.55	4.02	5.2522	0.8631	4.85	-12.6
14.5	5.71	4.02	6.1276	0.8398	5.31	-7.0
13.0	5.93	4.02	7.0030	0.8085	5.73	-3.3
11.5	6.34	4.02	7.8783	0.7569	6.10	-3.7

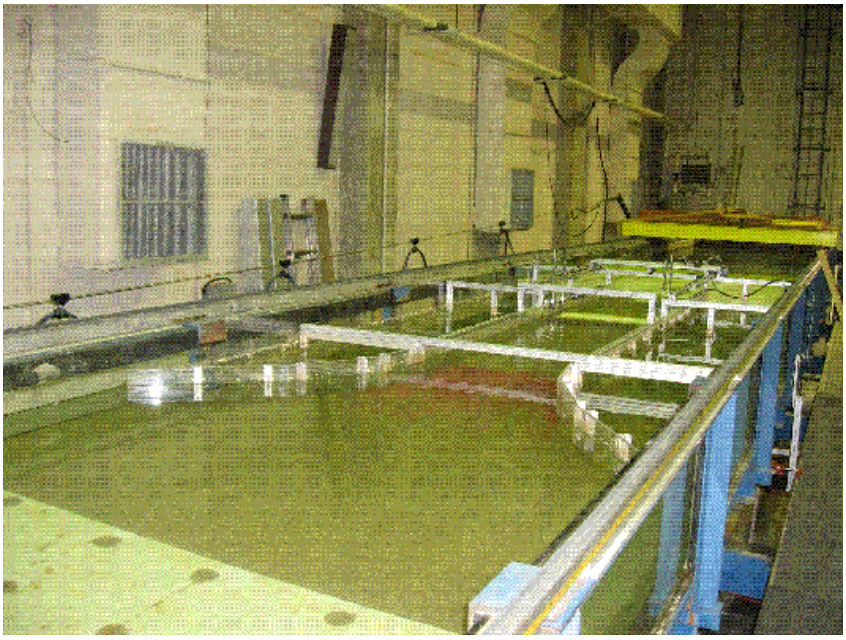

(a) Overview of the flume

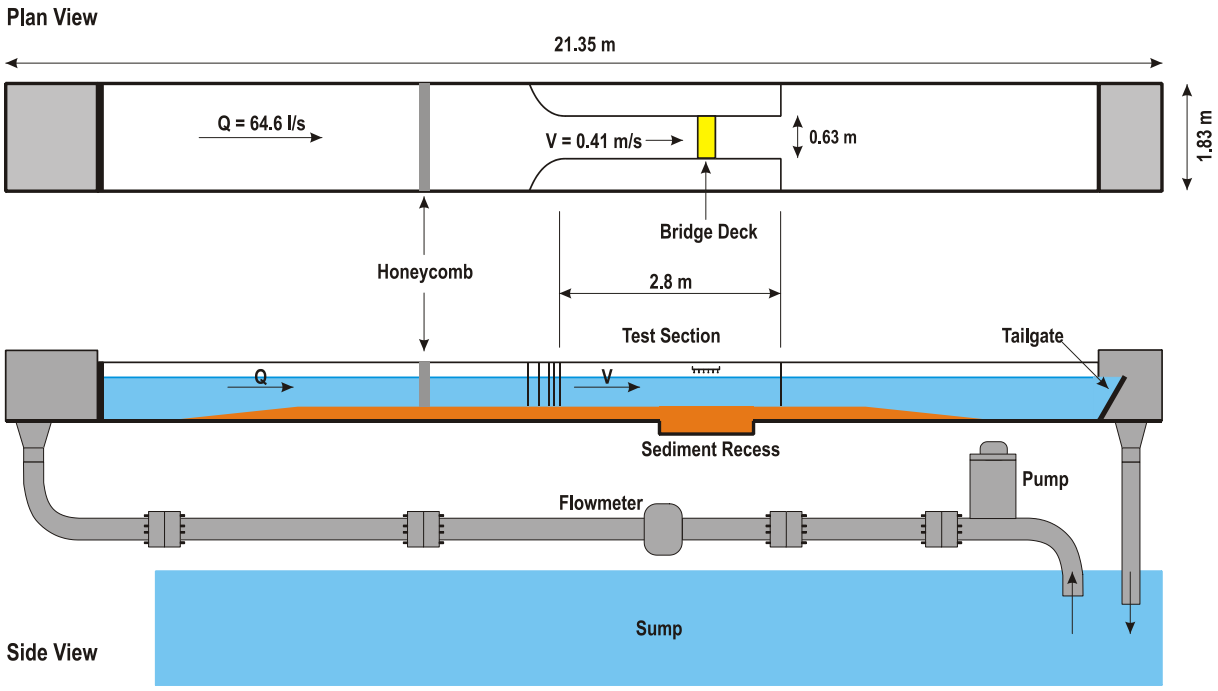

(b) The flume system

Fig. 1: Experimental apparatus

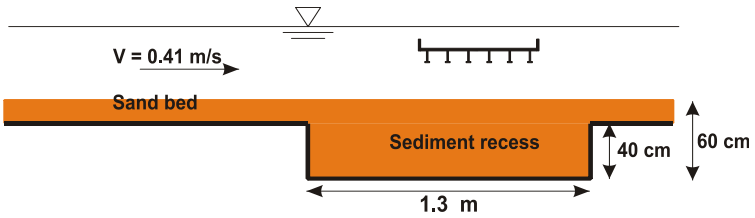

Fig. 2: Sand bed preparation in the test section

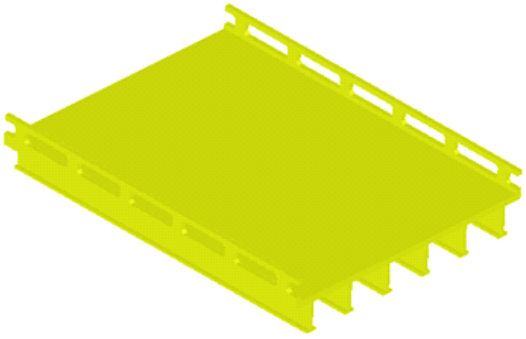

(a) The 6-girder deck in 3D view

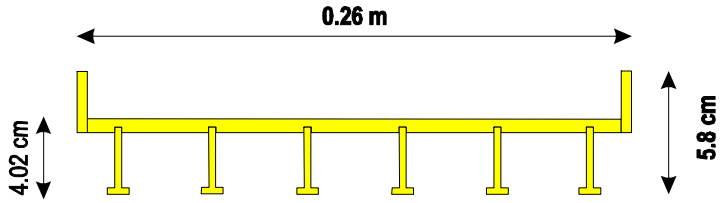

(b) Cross-section of the 6-girder deck

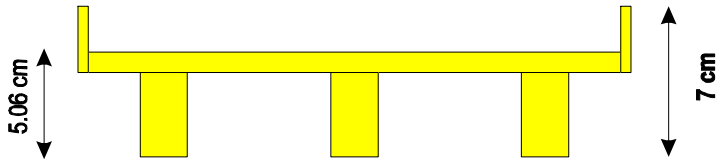

(c) Cross-section of the 3-girder deck

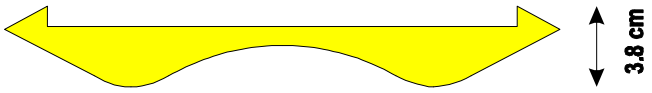

(d) Cross-section of the streamline deck

Fig. 3: Model decks of the experiments

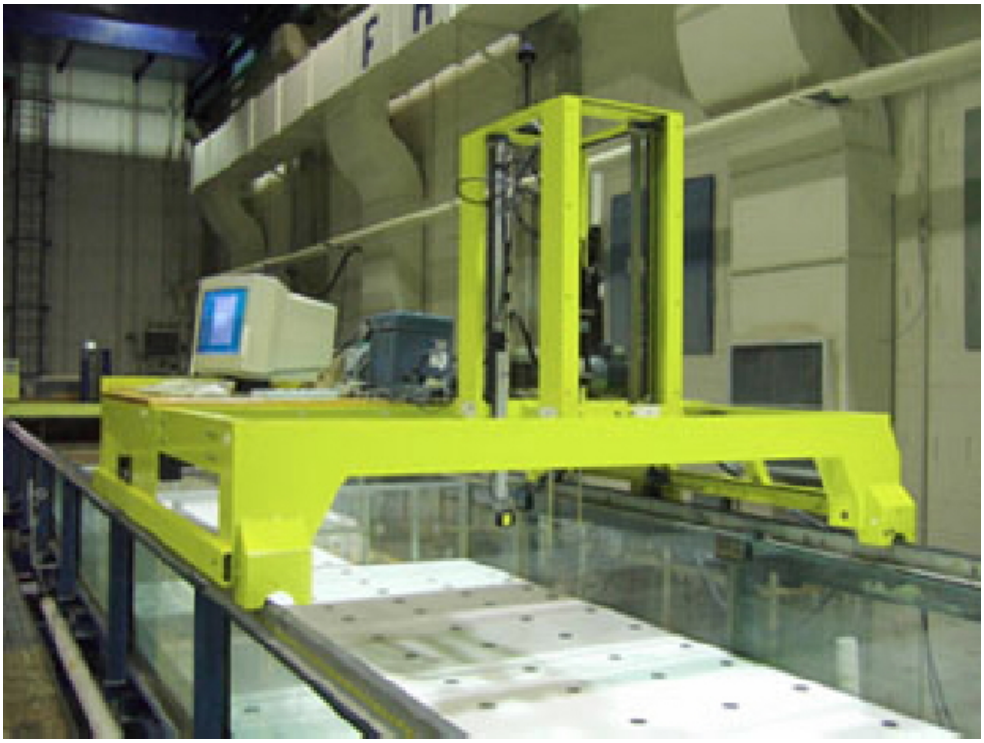

Fig. 4: The automated flume carriage fitted to the main flume.

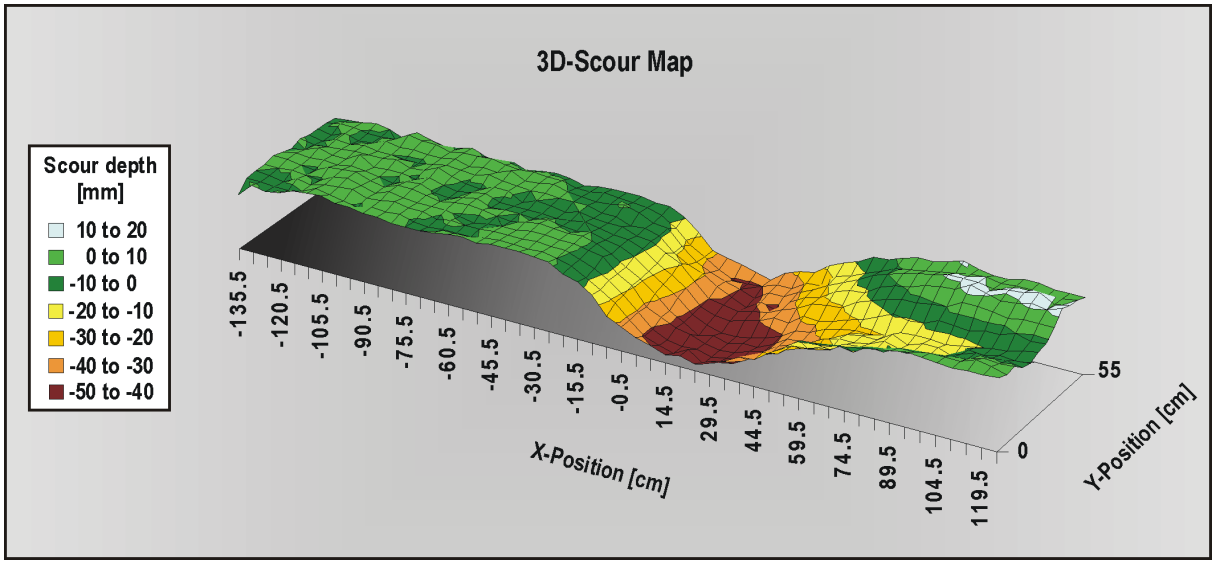

Fig. 5: A representative 3D scour map

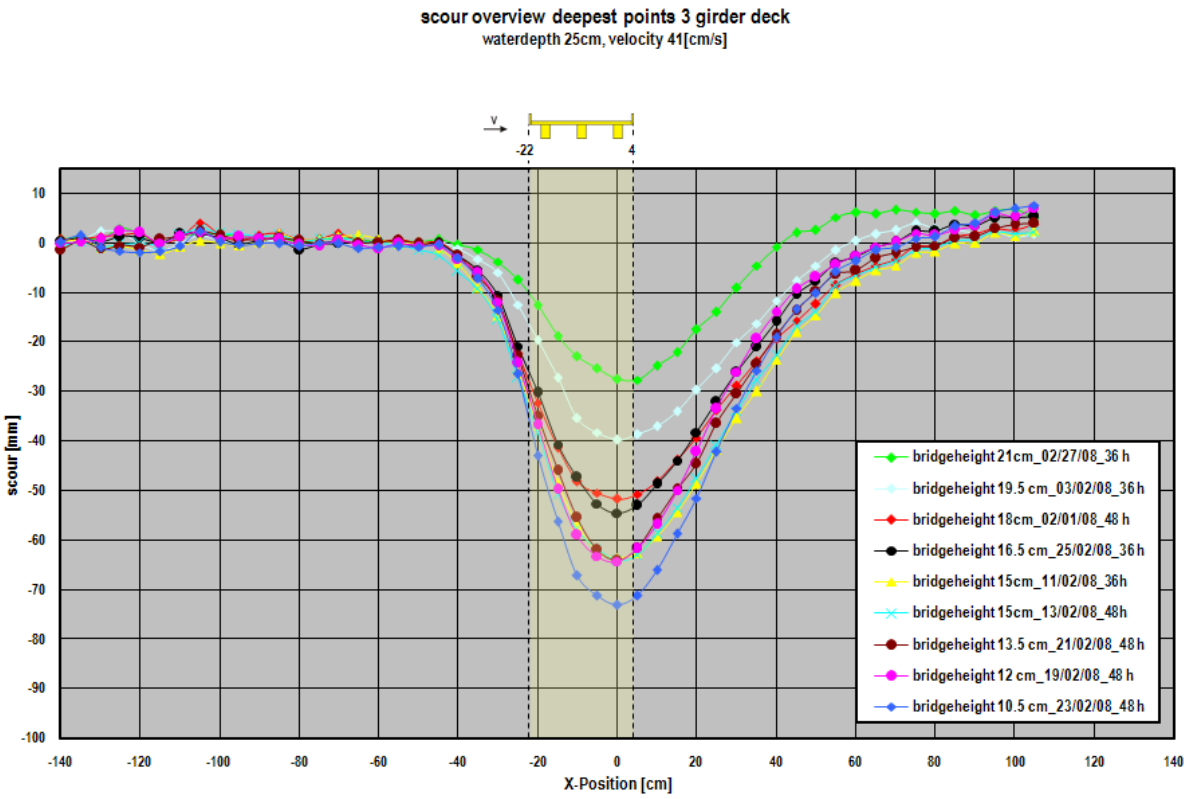

(a) Scour profiles under the 3-girder deck

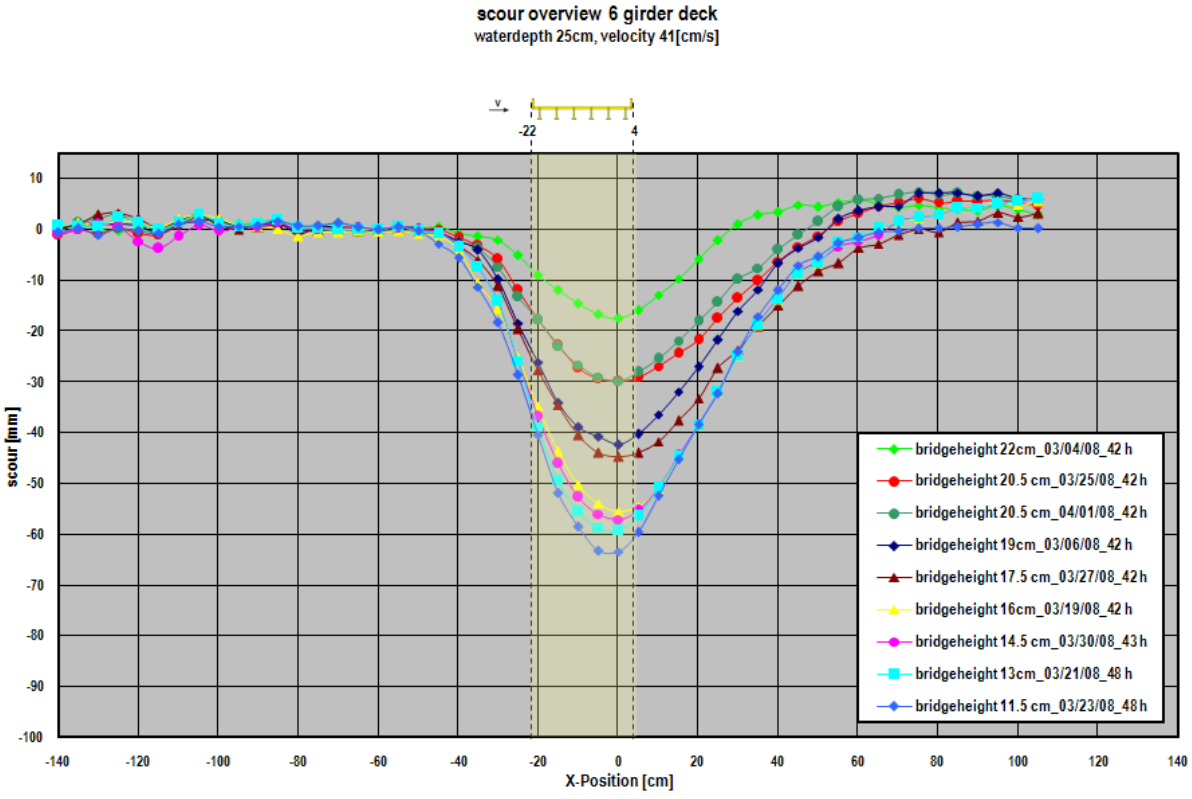

(b) Scour profiles under the 6-girder deck

Fig. 6: Measurements of scour profiles

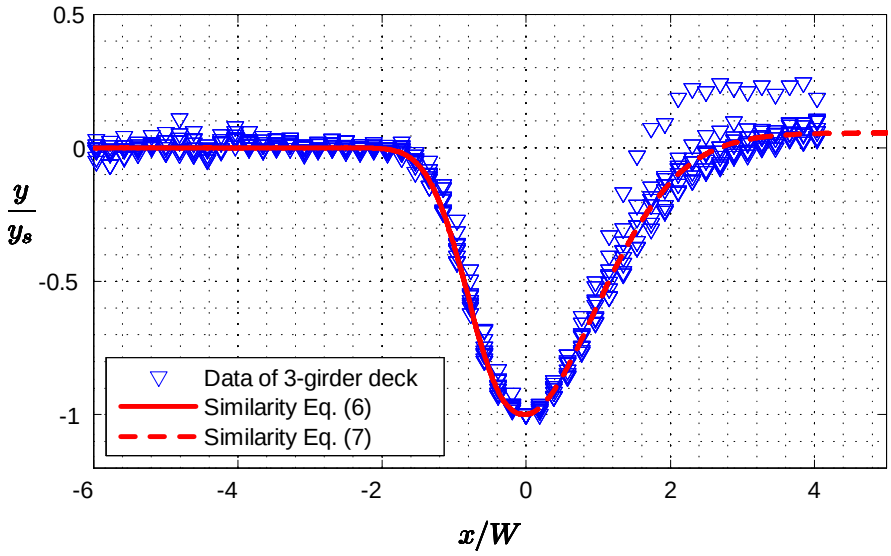

(a) Deck with 3-girders

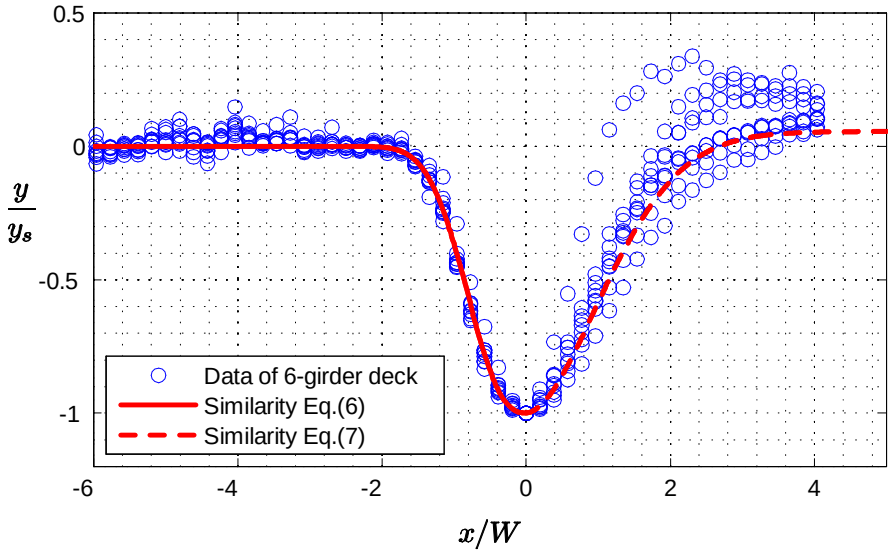

(b) Deck with 6-girders

Fig. 7: Similarity profile of scour holes

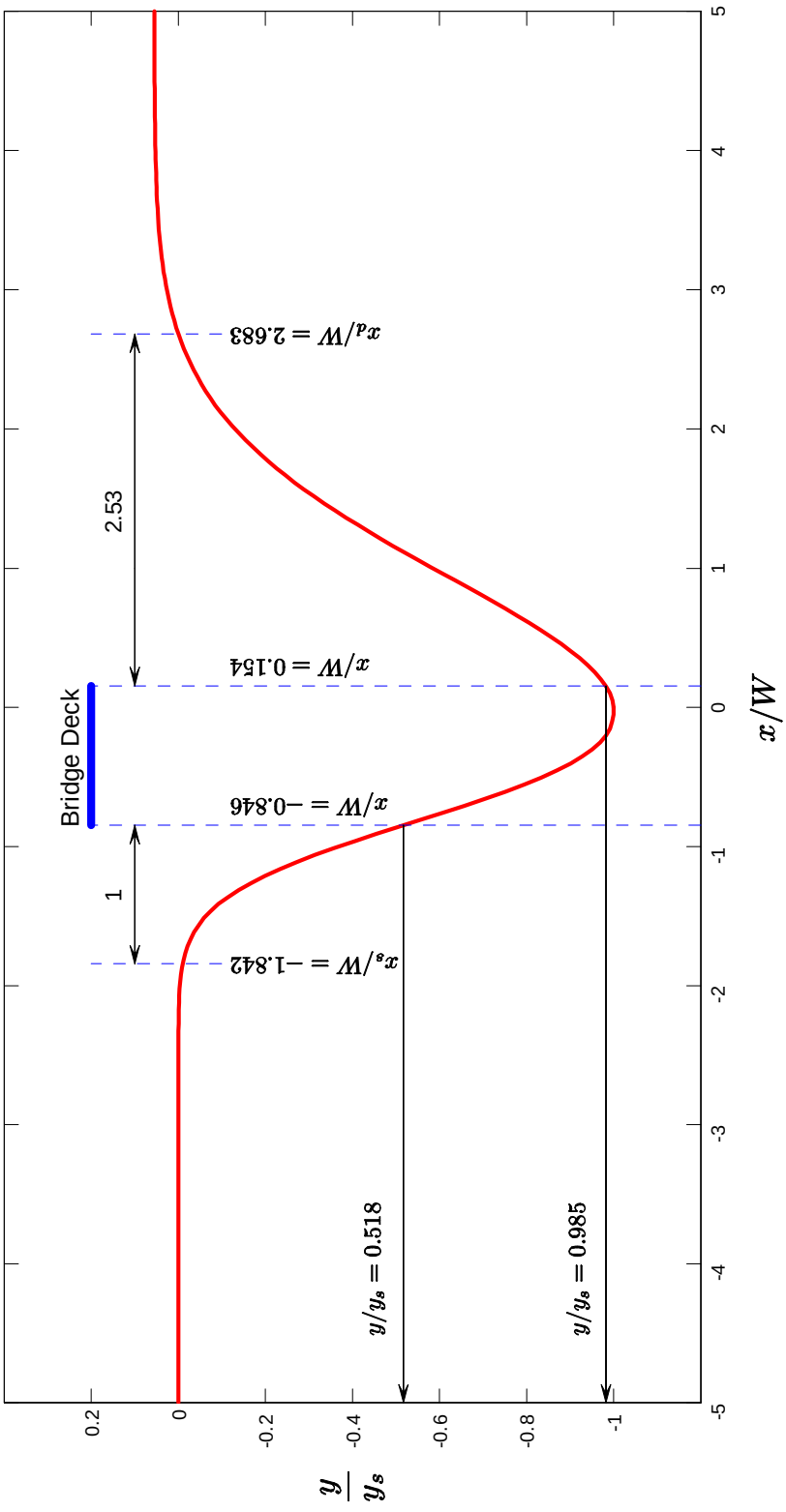

Fig. 8: Normalized scour profile with various characteristics

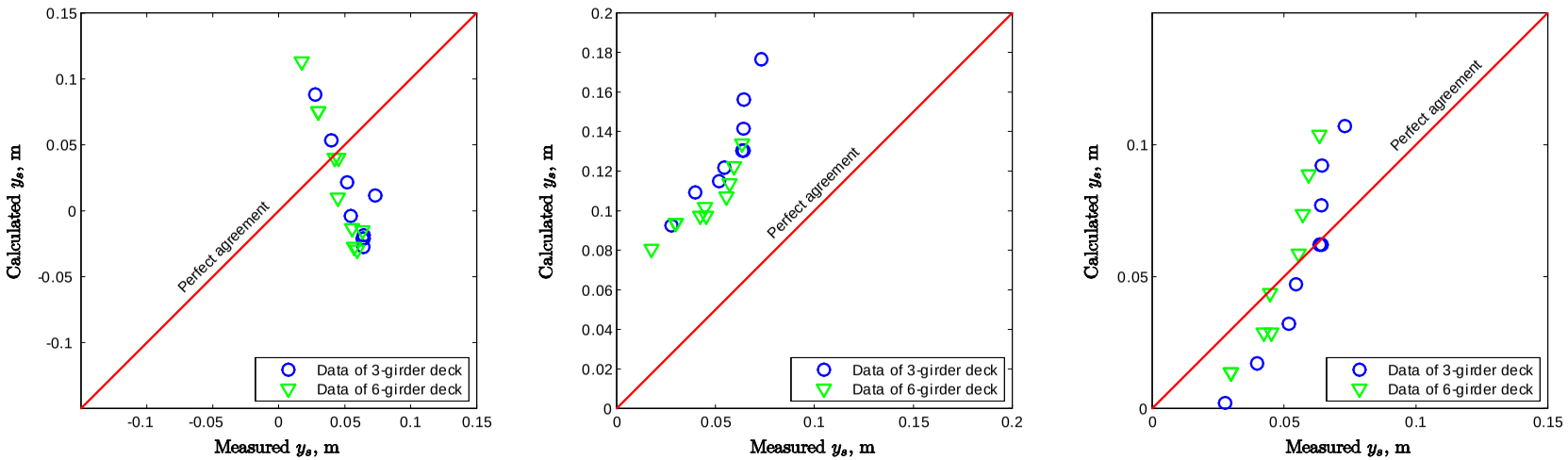

(a) The Arneson and Abt method (b) The Lyn method (c) The Umbrell et al. method

Fig. 9: Test of the existing methods for maximum scour depth

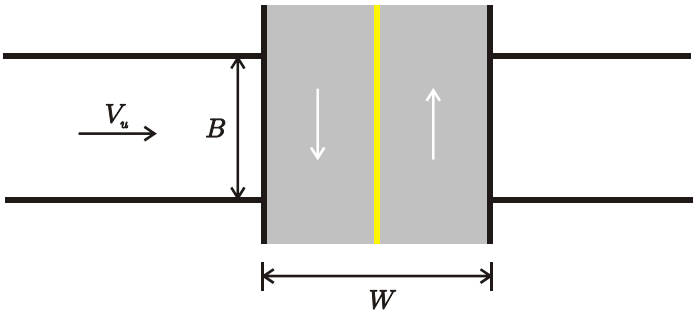

(a) Plan of a bridge crossing

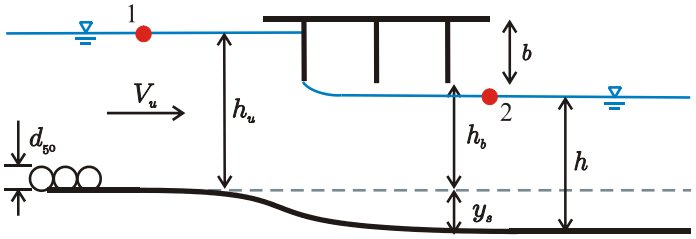

(b) Case 1: Inlet control orifice, $h_u/h_b < 1.1$

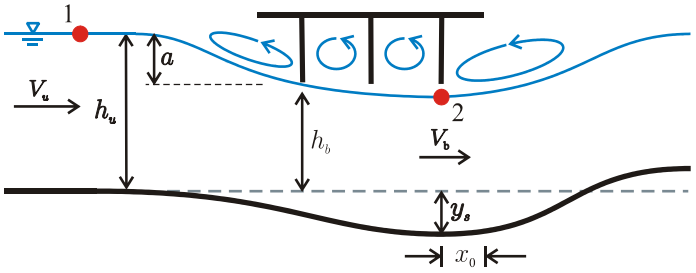

(c) Case 2: Outlet control orifice, $h_u/h_b \geqslant 1.1$

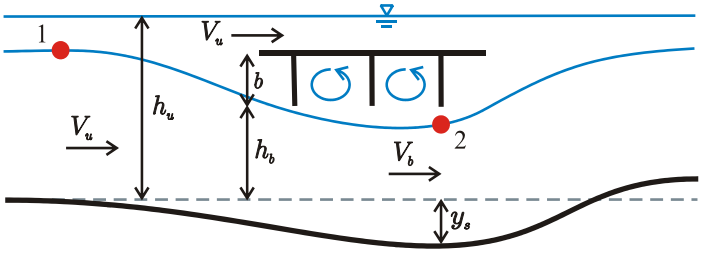

(d) Case 3: Combination of an orifice and a weir

Fig. 10: Scheme of flow through bridge

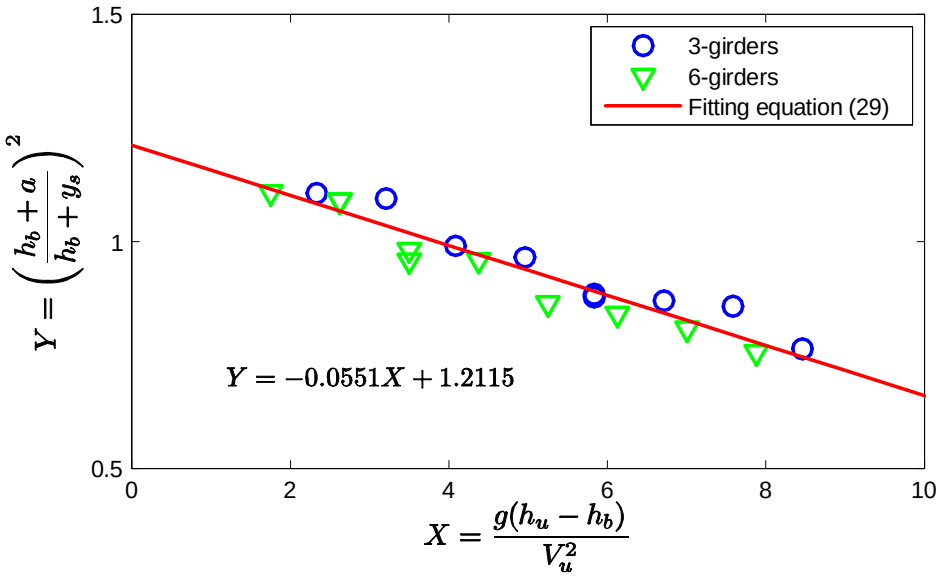

Fig. 11: Test of pressure flow scour equation

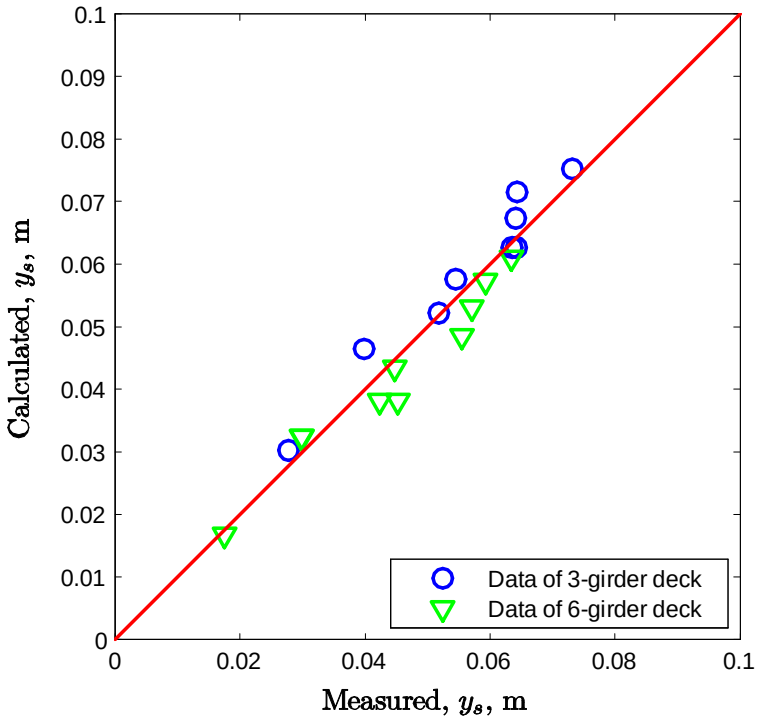

Fig. 12: Comparison of the proposed equation with the measured maximum scour depth

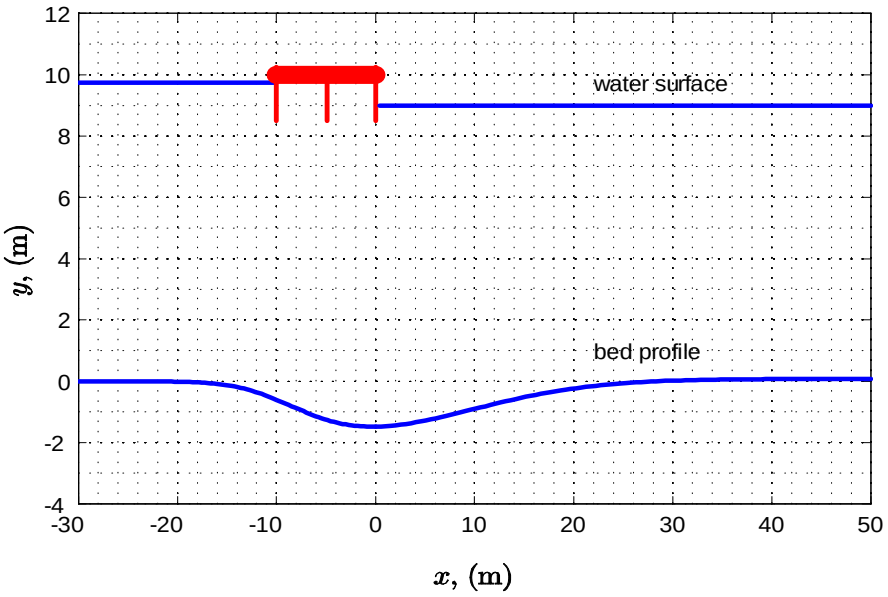

Fig. 13: Designed scour profile for the example problem

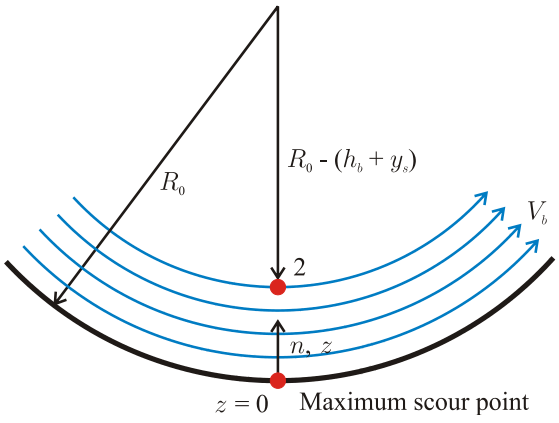

Fig. 14: Analysis of pressure under the bridge deck